Letters

Prehistoric Hertzian fracture of chert

Chert specimens which had been fractured by Stone Age Man into well defined Hertzian cones were found in the field. The geometric parameters of the cones were measured, and values of stress intensity factor required for the cone initiation were determined to be between 4.3 and 7.95 MN $m^{-3/2}$. The cones were generally produced by techniques responsible for asymmetric fractures, possibly by an elliptical indenter. Some of the cones were formed by excessive stresses and some by multi-stage processes.

The chert samples were collected in a small creek north of Mt. Safun 8 km east of Kziot in the Negev. Geologically, this chert is of the Middle Eocene period. It is a dense, fine-grained, high quality material (note Fig. 1), and differs from the chert of the Campanian period which is heterogeneous, and occasionally brecciated [1]. There are several clear indications suggesting that these cones have been produced by Stone Age Man. Although this chert is geologically widely spread in this region, conical cherts were found in an area confined only to a small creek, suggesting a prehistoric chert flaking industry. Fig. 2a and b show partly developed cones that look very similar to a typical fracture surface of a prehistoric stone tool ([2] Fig. 1). Furthermore, many flakes with fracture surfaces similar to a typical prehistoric flake described by Speth ([3] Figs. 4 and 5) were also associated with the conical cherts. Apart from above resemblances, the highly reproduced geometrical shapes of the Mt. Safun cherts are not expected to have been produced by natural phenomena.

Chert consists essentially of a network of microcrystalline quartz with a large number of micropores of 0.1 μm diameter [4]. As such it may be considered as a natural quartz ceramic. Mechanical Hertzian fracture techniques have been widely adopted for scientific investigation of highly brittle materials [5], mostly glass, but also fine-grained synthetic glass-ceramics [6, 7], as well as various silica modifications [8] and single crystals [9]. Hertzian fracture in glass has also been simulated by a thermal technique [10].

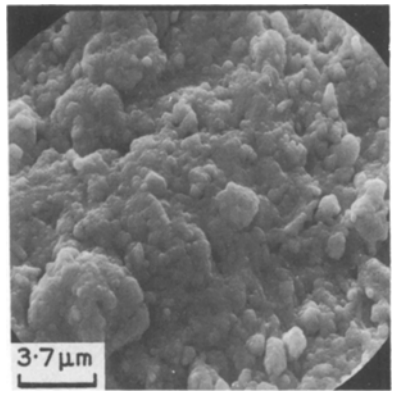

Figure 1 Scanning electron micrograph of Safun chert. Grains of about 1 μm are shown.

The Hertzian theory has been introduced into the field of ancient tool flaking by Kerkhof and Muller-Beck [11]. Previous treatments [2, 3, 11] were related to the Hertzian effect associated with partly developed cones. The present report, on the other hand, places more emphasis on the characterization of fully developed cones. The purpose of these cones is not yet clear. Crabtree [12] suggests that a cone formation was the Egyptian method for the perforation of beads. This problem, however, is beyond the scope of the present study.

Sample 1 in Fig. 2a shows a small partly developed cone. The hackle radiating from the cone is clear. Also, a thin transitional region of mist, about 0.5 mm thick is observed between the cone and the hackle. A highly developed series of concentric coarse ripples surrounding the cone is also observed. The fracture surface is asymmetrical; it shows a conical shape on the left and gradually converts into a plane shape on the right. Fig. 2b shows a small cone partly developed, and Fig. 2c a large cone not fully developed. The undeveloped parts of the cones are those parts of the original surface of the chert boulder that have not been removed. The initiation of the conic fracture in most samples investigated coincides with this surface chert, with the fracture deepening into the centre of it. This surface always shows a rough "skin". Such a skin which consists of large flaws (0.1 mm) suggests an elastic response analogous

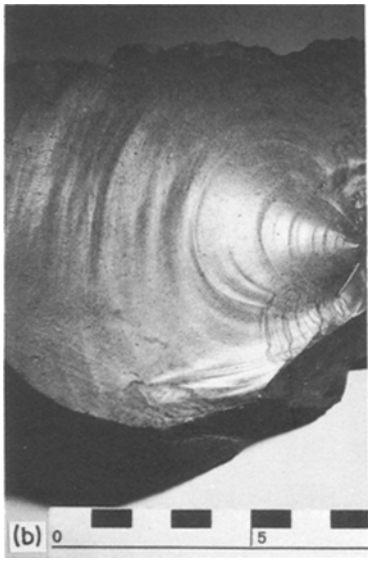

Figure 2 Sample 1 (a) shows a conical fracture partly developed. Part of the fracture surface continues to the right side from the conical surface into a plane surface. Sample 2 (b) shows a small cone partly developed with a radial prominent striation at the top of the cone, concentrical pronounced and delicate ripples, and a hackle region at the right-hand side of the cone. A large cone (sample 3), not fully developed, is shown in (c). Sample 4 (d) shows a cone produced in a concave surface.

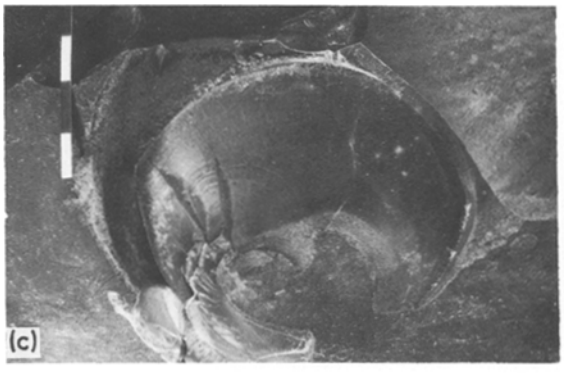

to a mechanism of a blunt indenter (hard sphere) as the cause of fracture [13].

It is astonishing to find in the field such well-defined Hertzian cones of various sizes, considering the fact that they were produced by methods far different from precise modern laboratory techniques. Several examples are shown in Fig. 3a to f. Various parameters of cones are summarized in Table I. The cone shown in Fig. 3a, like other cones investigated here, is asymmetrical, and the crack angle θ (the angle the cone crack makes with the cone axis – a normal to the flat original surface) differs on both sides of the axis. These crack angles are $\theta_l = 62.5^\circ$ and $\theta_s = 48^\circ$ and the average $\theta = 55.3^\circ \pm 1^\circ$.

Finnie and Vaidyanathan [14] have shown a dependence of the crack angle on both Poisson's ratio and the shape of indenter. The range of crack angle values measured in the present study for a material with a given Poisson's ratio (Table I) suggests a variety of techniques and/or conditions employed in producing the cones. (Note typically the elliptical "ring" cracks in two cones of Fig. 3e.) According to these values the crack angle which is commensurate with the Poisson's ratio, 0.16, of chert [2], (mean of 23 values) should be expected to be between 52° to 54°, which appears to be closer to the θ_s° values rather than θ_l° values (Table I) obtained for most fractured chert specimens. Hence, the mechanism responsible for the

TABLE I Parameters of prehistoric fracture of chert

Cone	θ_i°	θ_s°	$\theta^\circ(\pm 1^\circ)$ Average	$\alpha(\pm 1^\circ)$ Average	C(cm) Range	C(cm) Mean	K(MN m$^{-3/2}$)	D(cm)	d(cm)
1	62.5	48.0	55.3	34.7	3.99–5.06	4.52	7.95	7.65–7.86	0.49–0.79
2	67.0	52.5	59.8	30.2	3.37–4.49	3.93	5.8	8.57	1.23–1.92
3	67.5	53.5	60.0	30.0	2.81–4.64	3.72	5.6	9.17	1.55–2.64
4	67.0	56.0	61.5	28.5	5.10–8.00	6.55	7.9	–	1.43–1.77
5	62.5	62.5	62.5	27.5	3.35–6.09	4.72	5.4	10.37	2.29–3.25
6	61.5	54.5	58.0	32.0	4.72–6.00	5.36	7.5	11.23	1.82–2.11
7	66.0	55.0	60.5	29.5	1.99–2.63	2.31	4.3	–	–1.98

D are small and large (mostly large) diameters of the elliptical base of cones, and d are small and large diameters of elliptical ring cracks.

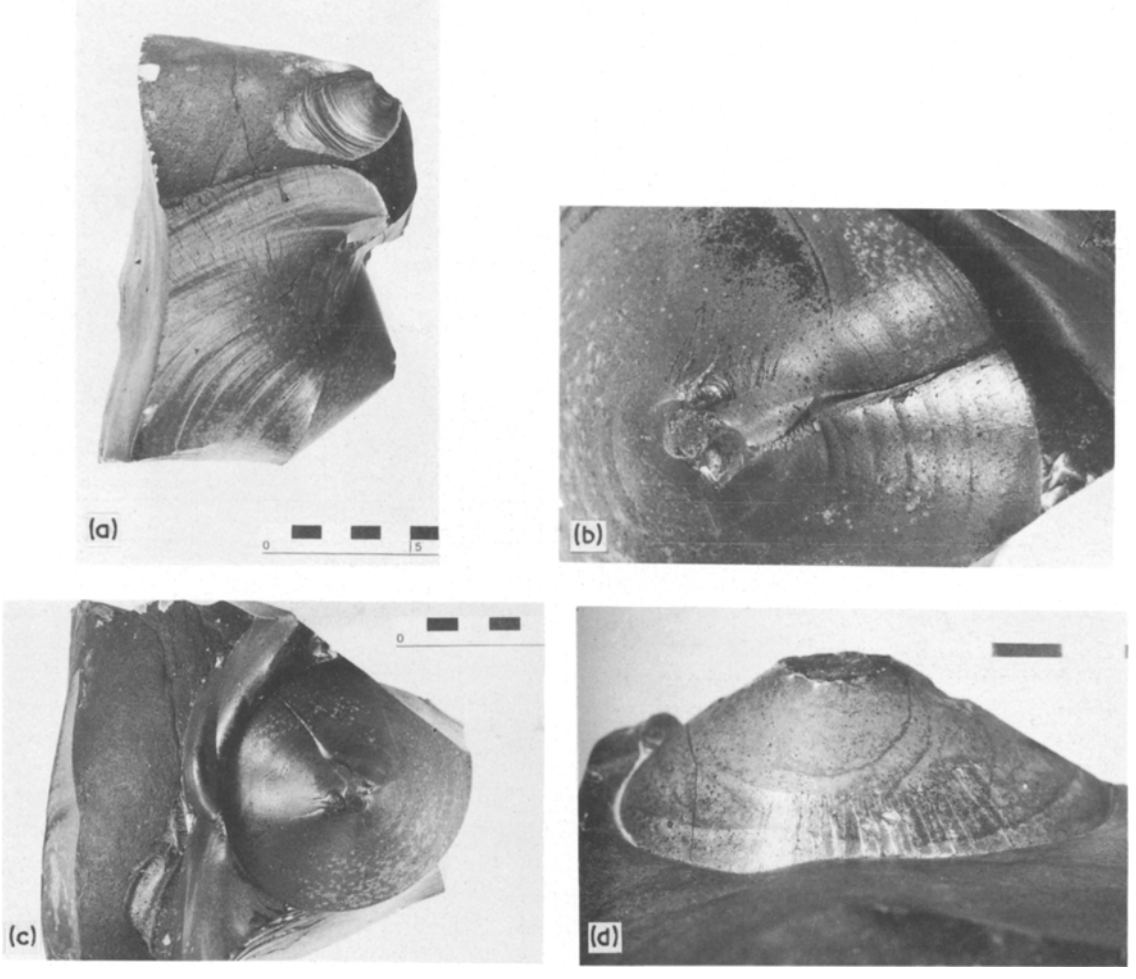

Figure 3 Sample 5 shows a Hertzian cone of chert (a) in profile, (b) surface view of cone fracture showing a prominent radial striation, small scars, spiral and concentric ripples, and (c) general surface view. Part of the cone has been removed, possibly while attempting to remove the mantle. Sample 6 (d) shows a series of radial striations on conical surfaces. Sample 7 (e) shows two separate cones together producing the circumference of a single cone. Sample 8 (f) shows a composite cone. Scales in Figs. 2 and 3 are in centimeter divisions.

fracture with a deviation of a circular ring crack to an elliptical crack and the asymmetry of the cone, is also responsible for the increase in the θ value beyond θ_s values. Thus, deviations may have been the result of one of three reasons; oblique application of load, shape of indenter or geometrical set-ups responsible for asymmetrical patterns of stress trajectories, expressed by irregularity of sample or application of load close to the edge of the sample. Fig. 2d demonstrates an attempt to produce a cone in a concave surface, rather than the flat surface normally investigated by modern scientists. As the shape and size of the initial elliptical crack is expected to be a reflection of the shape and size of the indenter, the possibility of an elliptical (large) indenter should not be discounted.

It is shown (Fig. 3b) that close to the apex of the cone, successive spiral ripples stop at a prominent radial striation, whereas at lower parts of the cone, concentric ripples continue on both sides of the individual striation. Both types of ripples represent up and down modulations of the cone fracture and have similar intensities. The spiral ripples were produced by elastic disturbances due to small scars near the cone apex. They resemble Wallner lines commonly observed on the fracture mirror planes of glass. About half way down the conical fracture, the spiral ripples transform into the concentric ripples. The prominent radial striation is a fracture scar indicating that an excessive stress has been applied while forming the cone [5]. This assumption is supported by the fact that the length of the cone fracture is about twenty times the radius of the circle of contact, i.e. the ring crack (Fig. 3a), rather than about three times [9] as under normal conditions.

A series of radial striations in the bases of various smooth cones, such as sample 6 (Fig. 3d) indicates a change in stress orientation in relation to the direction of fracture propagation, insinuating a continuous and/or multi-stage process. In Fig. 3d there is a short length of cone fracture relative to radius of circle. Sample 7 (Fig. 3e) shows two independent cones, which have the same periphery. These cones were produced by separate processes (very unlikely to be natural). Fig. 3f shows a composite cone (not quite complete). The cone axis seems to have changed its orientation at various stages of development and each stage is marked by a pronounced rib. Three such distorted ribs are observed which are differently oriented in relation to the cone axis, and result in a fracture surface with a wavy profile. Each rib is crowned by a series of short radial striations. In-between the various ribs, additional series of delicate ripples (Wallner lines) are observed. The composite cone was found to be not as common as the normal cone, and may represent a modified technique, thus emphasizing a series of load applications rather than a single process. The profile of the composite cone somewhat resembles a wavy cone produced by an induced thermal method [10].

The stress-intensity factor, K, required for the cone crack initiation may be derived from [13]:

$$K = \sigma(\pi C)^{1/2} \sin^2 \alpha \qquad (1)$$

where σ is the fracture strength, C the length of the conical crack and α is the inclination of the crack to the tensile axis. The latter two parameters are measurable on the investigated samples. The fracture strength may be derived from the Grif-

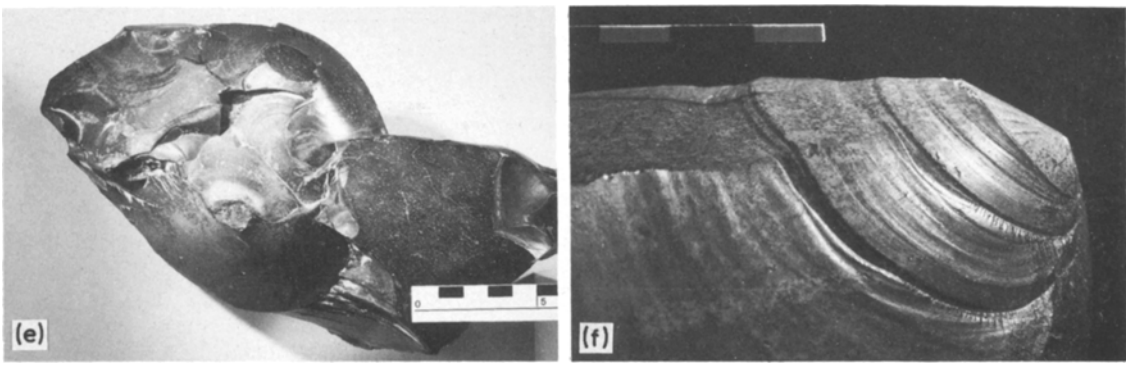

Figure 3 continued.

fith–Orowan–Irwin equation,

$$\sigma = Y\sqrt{(E\gamma c)}/\sqrt{a}, \qquad (2)$$

where Y is a geometrical constant (assumed to be 1) [15], E is the elastic modulus ($E = 9.83 \times 10^6$ psi $= 6.77 \times 10^4$ MN m^{-2}) [2], γc is the fracture energy ($\gamma c = 6.3$ J m^2 $= 63 \times 10^{-6}$ MN m^{-2}) which is the mean value for Tennessee (quartz) sandstone determined by two teams [16, 17], and $a = 0.1$ mm is the flaw size. The value obtained for σ is 65.3 MN m^{-2}, and values of K (given in Table I) fall between 4.3 and 7.95 MN m$^{-3/2}$ for the various specimens studied.

Acknowledgements

The author is indebted to Abraham Avigur who found the first sample which triggered this study and to Professor Reginald Shagam who encouraged the investigation of this subject. The Hertzian cones were photographed at the photographic laboratory of the university, and the SEM picture was photographed at the laboratory of the R & D Authority. The author wishes to thank Dr I. Gilead for introducing him to literature on prehistoric prehistory.

References

1. Y. KOLODNY, *Israel J. Earth. Sci.* **16** (1967) 57.
2. J. D. SPETH, *Amer. Antiquity* **37** (1972) 34.
3. J. D. SPETH and TEBIWA, *J. Idaho State Univ. Museum* **17** (1) (1974) 7.
4. W. A. DEER, R. A. HOWIE and J. ZUSSMAN, 'Rock Forming Minerals", Vol. 4 (Longman, London, 1971).
5. B. R. LAWN and R. WILSHAW, *J. Mater. Sci.* **10** (1975) 1049.
6. J. S. NADEAU and A. S. RAO, *J. Canad. Ceram. Soc.* **41** (1972) 63.
7. D. N. JARRETT and P. W. McMILLAN, *J. Phys. Instr.* 7 (1974) 913.
8. M. V. SWAIN, J. S. WILLIAMS, B. R. LAWN and Y. J. H. BEEK, *J. Mater. Sci.* 8 (1973) 1153.
9. B. R. LAWN, *J. Appl. Phys.* **39** (1968) 4828.
10. D. BAHAT, *J. Amer. Ceram. Soc.* in press.
11. F. KERKHOF and H. MULLER-BECK, *Glastech. Berich.* **42** (1969) 439.
12. D.E. CRABTREE and TEBIWA, *J. Idaho State Univ. Museum* **15** (2) (1972) 29.
13. B. R. LAWN, S. M. WIEDERHORN and H. H. JOHNSON, *J. Amer. Ceram. Soc.* **58** (9–10) (1975) 428.
14. I. FINNIE and S. VAIDYANATHAN, in "Fracture Mechanics of Ceramics", Vol. 1, edited by R.C. Bradt, D.P.H. Hasselmanard, F.F. Lange, (Plenum Press, New York, 1974).
15. S. W. FREIMAN, J. J. MECHOLSKY Jun. and R. W. RICE, *J. Amer. Ceram. Soc.* **58** (1975) 406.
16. T. K. PERKINS and W. W. KRECH, *Soc. Petrol. Engrs. J.* **6** (1966) 308.
17. M. FRIEDMAN, J. HANDIN and G. ALANI, *Int. J. Rock. Mech. Sci.* 9 (1972) 757.

Received 16 June
and accepted 24 September 1976

DOV BAHAT
Department of Geology and Mineralogy,
Ben-Gurion University of the Negev,
Beer Sheva, Israel

Comment on "Deformation in spinel"

As dislocation dissociation in metals is expected to influence slip in ionic and covalent crystals [1] at least at low temperatures, experimental attempts to derive the stacking fault energy (SFE) for these compounds are of fundamental interest. In the spinel $MgO(Al_2O_3)_n$, most of the work on SFE determination has been performed by Mitchell *et al.* [2]. The aim of this letter is to point out that their results are subject to some controversy, because all parameters influencing the final dislocation configurations have not been taken into account, resulting in possible erroneous conclusions.

In $MgO(Al_2O_3)_n$, perfect dislocations generally have $a/2\langle 1\,1\,0\rangle$ Burgers vectors. We have reported previously [3] that as a consequence of the dislocation dissocation into two partials with collinear Burgers vectors $a/4\langle 1\,1\,0\rangle$, dislocation network formation should involve climb unless the network geometry obeys precise criteria which, according to the Burgers vector $\boldsymbol{b}$ of the junction segment, are:

(1) $\boldsymbol{b} = a/2\langle 1\,1\,2\rangle$, the network is parallel to $\{1\,1\,1\}$ but the angles between its edges are 120°;

(2) $\boldsymbol{b} = a/2\langle 1\,1\,0\rangle$, the network is again parallel to $\{1\,1\,1\}$ but the angles may be 60° or 120°;

(3) $\boldsymbol{b} = a\langle 1\,0\,0\rangle$, the network is parallel to $\{0\,0\,1\}$, the angles are 90° or 45°.

In their analysis on plastic deformation in spinels, Mitchell *et al.* [2] stated that because glide has been observed to be activated on $\{1\,1\,1\}$